Dalton Transactions

Accepted Manuscript

ROYAL SOCIETY OF CHEMISTRY

www.rsc.org/dalton

Dalton Transactions

ARTICLE

Maleimide fused Boron-Fluorine complexes: Synthesis, Photophysical and electrochemical properties.

==Received 00th January 20xx,
Accepted 00th January 20xx

DOI: 10.1039/x0xx00000x

www.rsc.org/

Pranila B. Thale[†a], Pravin N. Borase[†a] and Dr. Ganapati S. Shankarling*[a].

Novel Boron Fluorine complex molecules were designed and synthesized using maleimide core moiety. Significant features such as large stoke shift, high quantum yield, long range absorption and emission wavelength were observed for these molecules. The lower LUMO level of these molecules indicates their potential application as electron transport materials. The optical band gap was calculated and compared by using UV- absorption edge, Density functional theory and electrochemical studies, reveal the charge transfer characteristics.

1. Introduction:

Boron dipyrromethene dyes[1] (BODIPY) are most important fluorescent dyes as they have wide application in the field of energy transfer cassettes[2], laser dyes[3], fluorescent indicators[4] bio labelling[5], photodynamic therapy[6] and in dye sensitized solar cells[7]. These dyes have spectacular photophysical properties such as high extinction coefficient, high fluorescence quantum yield, sharp absorption and fluorescence spectra. The photophysical properties can be easily tuned by structural modification which is an added advantage to meet diverse application. But, the main drawback in BODIPY dyes is their small Stokes shift which leads to self-quenching and measurement error due to excitation and scattering of light. They have compact $\pi - \pi$ stacking in solid state, which leads to greater molecular interaction resulting in fluorescence quenching[8]. Owing to above drawback, non-pyrrolic BODIPY analogue[9] have attracted considerable interest in recent years. They possess many advantages like readily available and cheap starting material, large stokes shift and good photostability. Thus, new types of fluorescent dyes based on borate complexes with N–B–O and N–B–N coordinate patterns have been efficiently synthesized. Only, few of these shows high emission efficiencies both in solution and solid[10] state. In recent years, incorporation of low electron density materials such as pyridine, quinoline into imide moiety to give boron fluorine complexes has been reported[11]. These complexes exhibit good optical properties, robust thermal stability and high electron transporting properties which is required for organic light emitting diodes.

Dye with solid state emissive properties and large stokes shift are in demand for practical application in molecular switches[12] and OLED[13]. Having this in mind, we have reported the synthesis and fluorescence properties of novel non-pyrrolic boron fluorine complexes based on maleimide derivatives. The synthesized complexes show broad absorption, high Stokes shift and intense fluorescence in solid as well as in the liquid state.

2. Experimental Section:

2.1 Materials:

All the chemicals were procured from Spectrochem and Merck chemicals. and were used without purification. The spectroscopic grade solvents were used in the study.

2.2 Instrumentation:

[a] Dyestuff Technology Department,
Institute of Chemical Technology, Mumbai 400019, India.
Tel: 91-22-33612708, Fax: +91-22-33611020
E-mail address: gsshankarling@gmail.com

† These authors contributed equally.

The ^{1}H NMR spectra were recorded on Bruker 300 MHz Spectrometer in $CDCl_3$ as a solvent in the presence of tetramethylsilane as internal standard. TLC was performed on TLC-Grade silica gel-G/UV 254 nm plate. The UV-visible spectra were recorded on PerkinElmer LAMBDA 25 UV/VIS spectrophotometer at room temperature using quartz cells with 1.0 cm path length. The fluorescence spectra was obtained on Varian Cary Eclipse Flourimeter. Time resolved fluorescence measurements were performed on a time correlated single photon counting system from IBH with excitation by a pulsed light emitting diode. The emission from the sample was collected at the right angle to the direction of excited beam, at a magic angle polarisation (54.7). The decay has been fitted to multiexponential functions by an iterative reconvolution method using JY Horiba IBH DAS v6.0 software[14].

3. Result and discussion:

3.1 Synthesis:

< Insert Scheme: 1>
< Insert Scheme: 2>
< Insert Scheme: 3>

The synthetic procedure of compounds BF1, BF21, BF3(I), BF3(II) are shown in scheme 1, 2 and 3. Condensation of compound 3a with 2-methylpyridine and 2-methylquinaldine was carried out with fused $ZnCl_2$ without any solvent in a sealed tube which gave compound 4 and 5 in good yield. The yield of the products were 47% and 52% respectively. The electron donating properties of 2-methylpyridine and 2-methylquinoline reduce the reactivity of second carbonyl group present at the opposite end of imide. Therefore, only mono substituted derivative is formed predominantly. Similarly, condensation of 3b with 2-methylpyridine gave compound 6 in 57% yield. Two isomers of compound 6 were, directly used for further reaction. The compound 4, 5 react with $BF_3.Et_2O$ in presence of N-ethyl-N,N-diisopropylamine in dichloromethane (DCM) for 24 h to give BF1, BF21 in yield of 42%, 44% respectively. Similarly, compound 6 was reacted with N-ethyl-N,N-diisopropylamine and $BF_3.Et_2O$ in DCM which gave two isomers. These were separated by column chromatography. The structure of BF3(I) isomer was confirmed by single X-ray crystallography data (fig 1). Since the solubility of BF3(II) was less, we could not obtain a single crystal of this compound. The structure of these compounds were fully characterized by different spectroscopic techniques such as HR-MS, ^{1}H NMR, ^{13}C NMR, ^{11}B NMR and elemental analysis.

< Insert Figure:1>

Figure1: ORTEP view of compound BF3(I)

3.1 X-ray crystal structure: By slow evaporation of the samples in chloroform and acetone, single crystal of BF3(I) suitable for X-ray diffraction analysis were obtained. The crystal is monoclinic in nature with space group $P2_1/n$. BF3(I) exhibits a slightly distorted tetrahedral geometry around boron atoms. The bond lengths of B4-F1, B4-F2, B4-N1 and B4-N2 were 1.382(2), 1.377(2), 1.605(2) and 1.528(2) $^{\circ}$A. Bond angle around B atom were ranging from 107.08(9)$^{\circ}$ to 112.2(1)$^{\circ}$. The crystal refinement data is shown in Table S2.

The crystal structure of BF3(I) shows interesting supramolecular interaction. The distance of supramolecular interaction are shown in Table S1. In packing diagram C(29)-H(29).....F(1), C(9)-H(9).....F(1), C(9)-H(9).....O(4), C(14)-H(14) .....F(2) interactions form zigzag like structure along c-axis (Fig.2). The non-covalent intermolecular interaction provide rigid structure to inhibit planar $\pi - \pi$ stacking in crystal structure because of which solid state fluorescence is observed.

< Insert Figure: 2 >

Figure 2: Packing diagram of BF3(I) (a) View along c-axis (b) View along a-axis.

3.2 Photophysical studies: The photophysical study of the Boron-Fluorine (BF) compounds are shown in Table 1. In DCM, BF1, BF3(I), BF3(II) show single absorption band at 403 nm, 402 nm, 402 nm respectively whereas, BF21 shows two absorption bands at 439 and 465 nm (fig.3a). The shift in absorption spectrum of BF21 is due to larger conjugation system of quinoline compared to pyridine in BF1. All the BF compounds shows intense and structured absorption bands. Minor solvatochromism effect (fig.S10-fig.S13 Supporting information) in the absorption band was observed which supports $\pi - \pi^*$ transition localized on the conjugated ring system.

< Insert Figure: 3>

Figure 3: Normalized (a) absorbance (b) emission spectra of BF compounds in DCM at 3µM concentration.

< Insert Figure: 4>

Figure 4: (a) Normalized absorption (A) and fluorescence spectra (F) of compound BF21 in acetone solution at five different concentrations (1) 1 µM (2) 1.5 µM (3) 2.0 µM (4) 2.5 µM (5) 3.0 µM with λ_{Ex} = 434 nm.
(b) Normalized emission spectra of BF compounds in solid state.

Table 1: Optical properties of BF compounds.

< Insert Table: 1 >

The photoluminescence of the BF compounds in different solvents was studied at room temperature. Excitation of these compounds shows green to blue fluorescence. The normalized emission spectra of the BF compounds in DCM at 3μM concentration are shown in fig 3(b). In DCM, BF1, BF3(I), BF3(II) show single emission band at 478 nm, 533 nm, 535 nm respectively whereas, BF21 shows two emission bands at 479 and 509 nm. The normalized spectra of BF21 (fig.4a) in acetone at five different concentrations show minimum overlap between absorbance and emission band leading to larger Stokes shift. The absorption and emission spectra display mirror symmetry, which indicate, the main bands correspond to S_0-S_1 transition. Whereas, BODIPY shows maximum overlap between absorbance and emission band. The Stokes shift, oscillator strength and quantum yield are the important properties of fluorescent compounds. Stokes shift indicates the difference in the properties and structure of the compound between ground state S_0 and first excited state S_1. The quantum yield (Φ_F) and energy yield of fluorescence (E_F) are listed in Table 2. Compared to smaller Stokes shift and insensitivity to the solvents of most BODIPY, larger Stokes shift and remarkable spectral changes are observed in the solvents for these compounds. The emission spectra of BF1, BF3(I), BF3(II) are solvent dependent. In toluene, BF1, BF3(I), BF3(II) showed emission maxima at 474nm, 501nm and 501nm respectively whereas, in a polar solvent like methanol, the compounds showed emission maxima at 520 nm, 568 nm and 573 nm respectively. These compounds display positive solvatochromic effect, decrease in fluorescence quantum yield and increase in Stokes shift with increase in the solvent polarity which explains the intersystem charge transfer (ICT) process. In polar solvent, the dipole moment of the molecule is enhanced upon excitation due to electron density redistribution. Hence the excited state is more stabilized in polar solvent due to stronger interaction with the dipole moment of solvents. Whereas, BF21 does not show solvatochromism, as there is small difference between ground state and excited state dipole moment of these molecule. This is illustrated by Lippert-Mataga equation later.

All BF compounds have noticeable solid-state emissions, which cover a wide range of 431-670 nm (fig.4b) while, BODIPY dyes show fluorescence in their solid state. Time resolved emission of these dyes were studied and fluorescence lifetime (τ) was determined by Time-correlated Single photon counting (TCSPC). These dyes gave monoexponential decay function with lifetime in the range of 1.08-2.86 ns (fig.S6-fig.S9 Supporting information)

Table 2: Quantum yield (Φ_F), energy yield of fluorescence (E_F) of BF compounds in different solvents (DCM, Acetone, Acetonitrile) and fluorescence lifetime (τ) in DCM.

< Insert table: 2>

In order to confirm charge transfer characteristic of these compounds, difference between the ground state and excited state dipole moment $(\mu_E - \mu_G)$ is calculated by Lippert and Mataga equation as follows[15].

$$(\nu_A - \nu_F) = \frac{2}{hc}(\Delta f)\frac{(\mu_E - \mu_G)^2}{a^3} + constant \ldots (1)$$

Where h is Planck's constant, c is velocity of light, (Δf) is solvent polarizability parameter and a is the Onsager radius of the dipole-solvent interaction sphere. The Onsager radius of the compound is estimated from ground state optimized structure using Turbomole-V6.6 program.

The solvent polarizability (Δf) is calculated by following equation (2) as shown in Table. S3 (supporting information).

$$(\Delta f) = \frac{\varepsilon - 1}{2\varepsilon + 1} - \frac{n^2 - 1}{2n^2 + 1} \ldots\ldots (2)$$

The graph of Stokes shift ($\nu_A - \nu_F$) v/s solvent polarizability (Δf) shows a linear relationship with the substantial slope which illustrate the ICT process fig 5(b). From the slope of the graph, the difference between the ground state and excited state dipole moment $(\mu_E - \mu_G)$ is calculated (Table 3). The dipole moment difference of BF3(I) and BF3(II) is more than BF1, BF21 which indicates that these compounds are more polarized in the excited state. The graph of Φ_F v/s (Δf) shows that the quantum yield decreases with increase in the solvent polarity fig 5(a). The near independence of Stokes shift on solvent polarity in BF21 with substantial lower value of the slope (Table.3) indicates that the permanent dipole moment (if any) are similar in the ground and excited state.

Table 3: Ground state and excited state dipole moment difference $(\mu_E - \mu_G)$ of BF compounds.

< Insert Table: 3>

<Insert Figure: 5>

Fig 5(a): Plot of Φ_F v/s (Δf) of BF compounds (DCM, Acetone, Acetonitrile). (b) Plot of Stokes shift ($v_A - v_F$) v/s solvent polarizability (Δf) of BF compounds in various solvents.

3.3 Electrochemical studies: The electrochemical properties of BF compounds were determined by cyclic voltammetry in dichloromethane (DCM) at a scan rate of 100 mVs^{-1} using tetrabutyl ammonium hexafluorophosphate ($TBAPF_6$) as supporting electrolyte. Potential was standardized with ferrocene-ferrocenium couple (Fc/Fc^+) as an internal reference vs $Ag/AgNO_3$. The cyclic voltammograms of all compounds are illustrated in fig 6. and their electrochemical properties are summarized in Table 3. The corresponding energy levels of highest occupied molecular orbital (HOMO) and lowest unoccupied molecular orbital (LUMO) for BF compounds are calculated from the onset of the oxidation and reduction peaks. As predicted in the Table.4, the calculated HOMO values were ranging from -6.16 to - 6.02 eV which are lower than those of BODIPY (-5.45eV) and Alq_3 (-5.7 eV). The electron affinity values (LUMO level) were –3.26 to - 2.84 eV which are close to the LUMO level of BODIPY (-3.05 eV)[16] and Alq_3 (-2.8 eV)[17]. From the above studies, it is clear that BF compounds have better electron accepting features and have potential as an electron transport material in OLEDs. For better understanding, we have compared the values of HOMO, LUMO level, band gap by DFT and UV studies (Table.4). The results are in good agreement with the experimental and theoretical calculations.

< Insert Figure: 6>

Figure 6: Cyclic voltammograms of BF compounds measured in DCM solution, containing 0.1 M $TBAPF_6$ at 20°C. Ferrocene was used as an internal standard, and potential was calculated relative to the SCE assuming $E_{1/2}$ (Fc/Fc^+) to be +0.43.

Table 4: Electronic states (HOMO/LUMO levels) values and energy gap (eV).

<Insert Table 4:>

V_{cv}: Value from cyclic voltammetry; V_{ca}: Value from MO calculation; v_{uv}= Value obtained from UV-vis absorption edge studies.

Thermal stability of BF compounds was investigated by thermo gravimetric analysis (TGA) as shown in fig.S14 (Supporting information). Thermal stability is defined as temperature up to which 95% of the composition of the compound remains stable. Stepwise ramping up to 600°C at 10°C/minute was performed in nitrogen atmosphere. The change in weight of the compound was measured as a function of temperature. The Compound BF1, BF21 were stable up to 275°C whereas, BF3(I), BF3(II) were stable up to 325°C because of the presence of naphthyl ring on the anhydride core moiety.

In order to investigate the photo stability, 10 ppm solutions of BF compounds in acetonitrile were subjected to UV irradiation (254 nm, 0.025W/cm^2) for 500 min (fig.7). The kinetics of photo degradation was monitored spectroscopically. It was found that there is no change in optical density for all the compounds under study. This indicates that they have good photo stability[18] which is important for their application in photo electronics.

< Insert Figure 7:>

Figure 7: Change in optical density of BF compounds v/s time (min) on irradiation with UV light (0.025W/cm^2).

3.4 Theoretical studies: To understand the electronic properties, molecular orbital calculation were carried out by Turbomole-V6.6 program using density functional theory (DFT) (B3LYP as functional and def-SVP basis set)[19]. The ground state electron density distribution of HOMO and LUMO are illustrated in fig. 8 and the energy difference is presented in Table 4. The π electron densities in HOMO of BF1 and BF21are spread over part A while, their π electron densities in their LUMO are mainly localized on the part B. The electron densities in HOMO of BF3(I), BF3(II) are localized on the electron rich Napthyl ring part A whereas, electron densities in the LUMO level are entirely shifted to part B. Therefore, intermolecular charge transfer from part A to part B in BF compounds can be explained, which could partly explain their broad absorption band and larger stokes shift. The calculated HOMO-LUMO band gap of BF1 was larger than that of BF21 which is consistent with the trend observed in the spectra.

< Insert Figure: 8 >

Figure 8: Diagram showing HOMO and LUMO level of BF compounds.

4. Conclusion: In summary, we have successfully synthesized novel Boron-fluorine molecules with longer wavelength absorption and emission by introducing methylpyridine and methylquinoline group at the carbonyl position of maleimide derivative. The synthesized derivatives have longer absorption, emission wavelength, high quantum yield and large Stokes shift. Intense solid state fluorescence, thermally robust nature and low LUMO level of

synthesized molecules indicate their potential for use in OLED material.

Acknowledgment:

Authors are greatly thankful to Prof. Anindya Datta IIT, Bombay for providing fluorescence decay measurement instrument facility. Authors are also thankful to UGC-SAP, Technical Education Quality Improvement Programme (TEQUIP), for providing financial assistance and SAIF IIT, Bombay for recording ^{1}H NMR and elemental analysis.

Notes and references:

(1) (a) A. Loudet, K.Burgess, *Chem. Rev.*, 2007**,** **107**, 4891-4932. (b) G. Ulrich, R. Ziessel, A. Harriman, *Angew. Chemie - Int. Ed.,* 2008, **47**, 1184-1201. (c) L. C. D. D. L. Rezende, S. Emery, F. Emery, *Orbital-The Electron. J. Chem.,* 2013, **5***,* 62-83. (d) Y.Ni, J. Wu, *Org. Biomol. Chem.,* 2014, **12**, 3774-3791.

(2) M.Benstead, G. H. Mehl, R. W. Boyle, *Tetrahedron,* 2011, **67**, 3573-3601.

(3) T. L. Arbeloa, F. L. Arbeloa, I. L. Arbeloa, I. García- Moreno, a Costela, R. Sastre, F. Amat-Guerri, *Chem. Phys. Lett.,* 1999, **299**, 315-321.

(4) (a) J. L. Bricks, A. Kovalchuk, C. Trieflinger, M. Nofz, M. Büschel, A. I. Tolmachev, J. Daub, K. Rurack, *J. Am. Chem. Soc.,* 2005, **127**, 13522–13529. (b) K. Yamada, Y. Nomura, D. Citterio, N. Iwasawa, K. Suzuki, *J. Am. Chem. Soc.,* 2005, **127**, 6956–6957. (c) A. Coskun, E. U. Akkaya, *J. Am. Chem. Soc.,* 2006, **128**, 14474–14475. (d) A. Coskun, M. D. Yilmaz, E. U. Akkaya, *Org. Lett.,* 2007, **9**, 607–609. (e) N. Boens, V. Leen, W. Dehaen, *Chem. Soc. Rev.,* 2012, **41**, 1130–1172.

(5) M. Sameiro, T. Gonçalves, *Chem. Rev.*, 2009, **109**, 190–212.

(6) A. Kamkaew, S. H. Lim, H. B. Lee, L. V. Kiew, L. Y. Chung, K. Burgess, *Chem. Soc. Rev.*, 2012, **42**, 77–88.

(7) (a) S. Erten-Ela, M. D. Yilmaz, B. Icli, Y. Dede, S. Icli, E. U. Akkaya, *Org. Lett.*, 2008, **10**, 3299–3302. (b) T. Rousseau, A. Cravino, T. Bura, G. Ulrich, R. Ziessel, J. Roncali, *Chem. Commun. (Camb).*, 2009, 1673–1675.

(8) (a) T. Ozdemir, S. Atilgan, I. Kutuk, L. T. Yildirim, A. Tulek, M. Bayindir, and E. U. Akkaya, *Org. Lett.*, 2009, **11**, 2105–2107. (b) D. Zhang, Y. Wen, Y. Xiao, G. Yu, Y. Liu, and X. Qian, *Chem. Commun. (Camb).*, 2008, 4777–4779. (c)H. Lu, Q. Wang, L. Gai, Z. Li, Y. Deng, X. Xiao, G. Lai, and Z. Shen, *Chem. - A Eur. J.*, 2012, **18**, 7852–7861. (d) L. Gai, H. Lu, B. Zou, G. Lai, Z. Shen, and Z. Li, *RSC Adv.*, 2012, **2**, 8840.

(9) D. Frath, J. Massue, G. Ulrich, and R. Ziessel, *Angew. Chemie - Int. Ed.*, 2014, **53**, 2290–2310.

(10) (a) W. Li, W. Lin, J. Wang, and X. Guan, *Org. Lett.*, 2013, **15**, 1768–1771. (b) D. Frath, A. Poirel, G. Ulrich, A. De Nicola, and R. Ziessel, *Chem. Commun.*, 2013, **49**, 4908. (c) J. Massue, D. Frath, P. Retailleau, G. Ulrich, and R. Ziessel, *Chem. - A Eur. J.*, 2013, **19**, 5375–5386. (d) K. Benelhadj, J. Massue, P. Retailleau, G. Ulrich, and R. Ziessel, *Org. Lett.*, 2013, **15**, 2918–2921.

(11) (a) Y. Zhou, Y. Xiao, D. Li, M. Fu, *J. Org. Chem.*, 2008, **73**, 1571–1574. (b) J. Feng, B. Liang, D.Wang, L. Xue, X. Li, *Org. Lett.*,2008, **10**, 4437-4440.

(12) S. J. Lim, B. K. An, D. J. Sang, M. A. Chung, and Y. P. Soo, *Angew. Chemie - Int. Ed.*, 2004, **43**, 6346–6350.

(13) (a) H. Sasabe, J. Kido, *Chem. Mater.*, 2011, **23**, 621–630. (b) a. Hepp, G. Ulrich, R. Schmechel, H. Von Seggern, R. Ziessel, *Synth. Met.*, 2004, **146**, 11–15. (c) S. J. Yeh, M. F. Wu, C. T. Chen, Y. H. Song, Y. Chi, M. H. Ho, S. F. Hsu, C. H. Chen, *Adv. Mater.*, 2005, **17**, 285–289. (d) S. W. Wen, M. T. Lee, C. H. Chen, *IEEE/OSA J. Disp. Technol.*,2005, **1**, 90–99.

(14) D. Panda, S. Khatua, and A. Datta, *J. Phys. Chem. B*, 2007, **111**, 1648–1656.

(15) M. Shaikh, J. Mohanty, P. K. Singh, a. C. Bhasikuttan, R. N. Rajule, V. S. Satam, S. R. Bendre, V. R. Kanetkar, H. Pal, *J. Phys. Chem. A*, 2010, **114**, 4507–4519.

(16) Y. Zhou, Y. Xiao, S. Chi, X. Qian, *Org. Lett.*, 2008, **10**, 633–636.

(17) P. E. Burrows, Z. Shen, V. Bulovic, D. M. McCarty, S. R. Forrest, J. A. Cronin, M. E. Thompson, *J. Appl. Phys.*, 1996, **79**, 7991-8006.

(18) (a) T. Konstantinova, R. Lazarova, A. Venkova, V. Vassileva, *Polym. Degrad. Stab.*, 2004, **84**, 405–409. (b) T. Konstantinova, R. Lazarova, V. Bojinov, *Polym. Degrad. Stab.*, 2003, **82**, 115–118.

(19) (a) TURBOMOLE V6.6 (2014), A Development of University of Karlsruhe and Forschungszentrum Karlsruhe GmbH, 1989–2007, TURBOMOLE GmbH, since 2007, available from http://www.turbomole.com (b) O.T. Ahlrichs, R. Ahlrichs, Efficient molecular numerical integration schemes, J. Chem. Phys. 1995,**102**, 346–354. (c) M. Von Arnim, R. Ahlrichs Performance of parallel TURBOMOLE for density functional calculations, J. Comput. Chem. 1998, **19**, 1746-1757.

Figure Caption:

Scheme 1:

Scheme 2:

Scheme 3:

Figure1: ORTEP view of compound BF3(I).

Figure 2: Packing diagram of BF3(I) (a) View along c-axis (b) View along a-axis.

Figure 3: Normalised (a) absorbance (b) emission spectra of BF compounds in DCM at 3μM concentration.

Figure 4: (a) Normalised absorption (A) and fluorescence spectra (F) of compound BF21 in acetone solution at five different concentrations (1) 1 μM (2) 1.5 μM (3) 2.0 μM (4) 2.5 μM (5) 3.0 μM with λ_{Ex} = 434 nm.

(b) Normalised emission spectra of BF Compounds in solid state.

Fig 5: (a) Plot of Φ_F v/s (Δf) of BF compounds (DCM, Acetone, Acetonitrile). (b) Plot of Stokes shift ($\nu_A - \nu_F$) v/s solvent polarizability (Δf) of BF compounds in various solvents.

Figure 6: Cyclic voltammograms of BF compounds measured in DCM solution, containing 0.1 M $TBAPF_6$ at 20°C. Ferrocene was used as an internal standard, and potential was calculated relative to the SCE assuming $E_{1/2}$ (Fc/Fc^+) to be +0.43.

Figure 7: Change in optical density of BF compounds v/s time (min) on irradiation with UV light (0.025W/cm^2).

Figure 8: Diagram showing HOMO and LUMO level of BF compounds.

Scheme 1

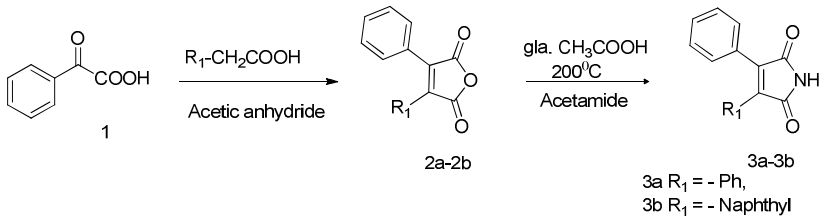

Scheme 2:

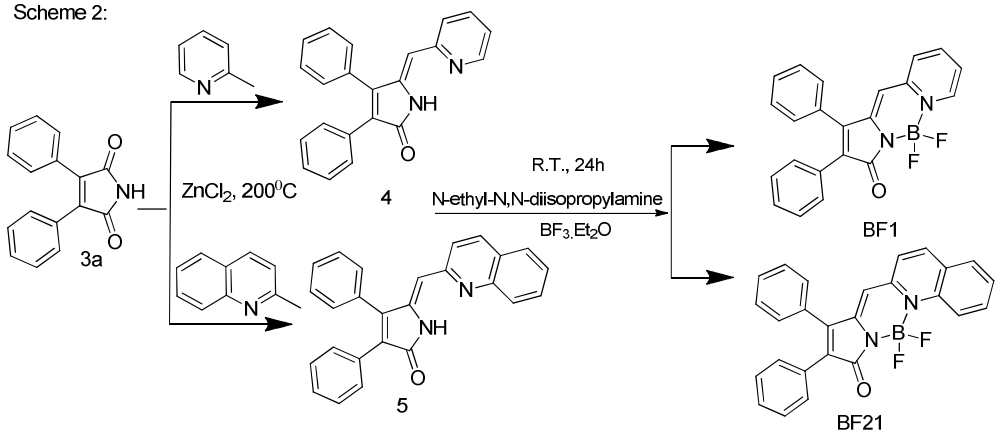

Scheme 3:

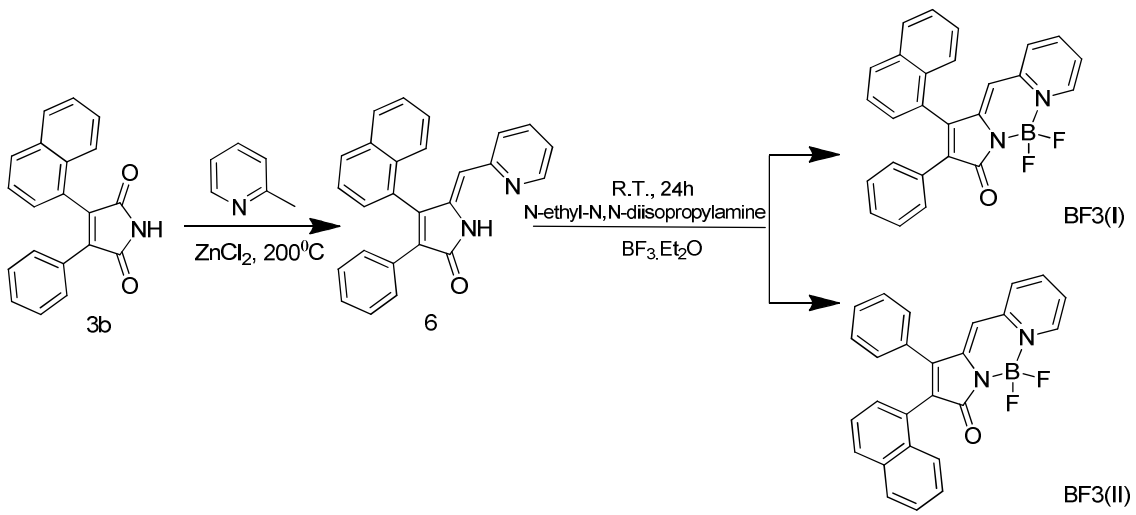

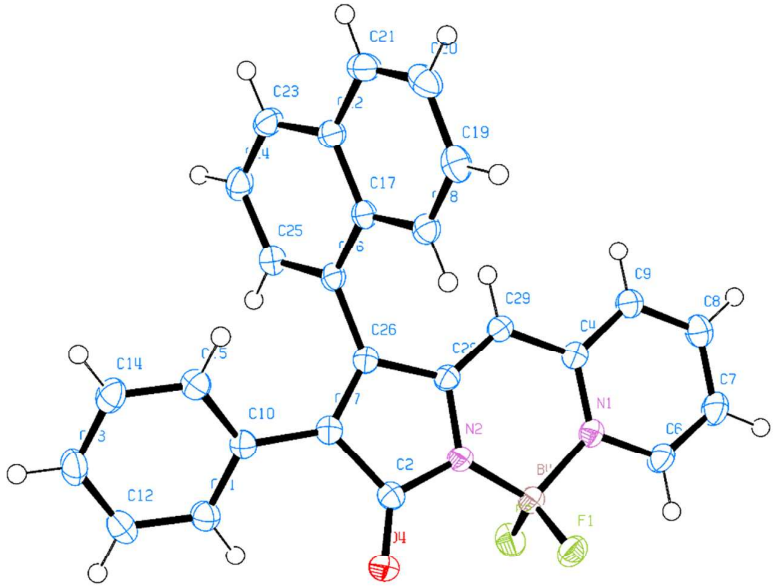

Figure1: ORTEP view of compound BF3(I).

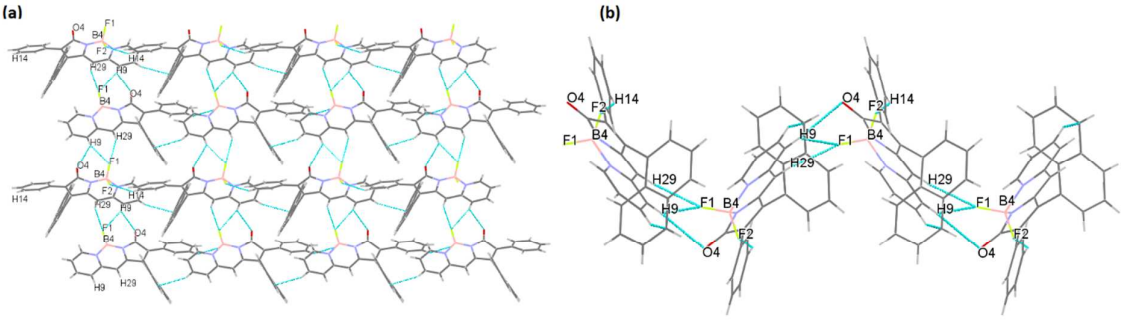

Figure 2: Packing diagram of BF3(I) (a) View along c-axis (b) View along a-axis.

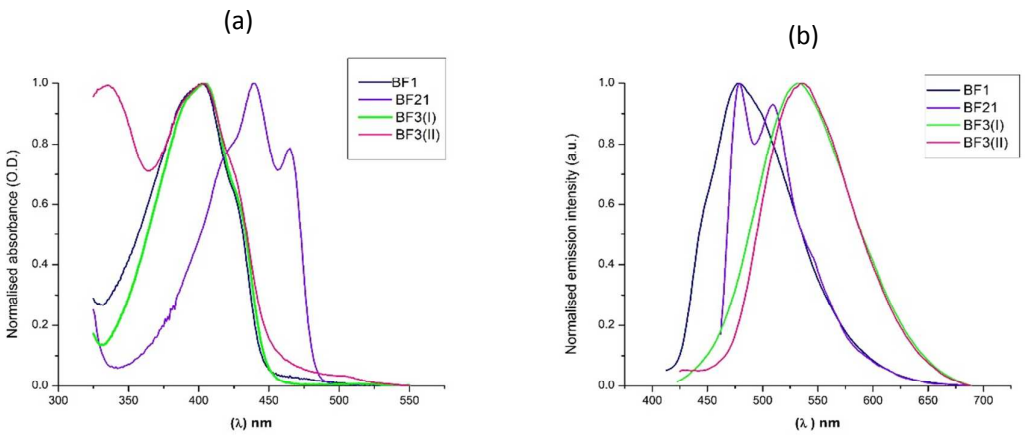

Figure 3: Normalised (a) absorbance (b) emission spectra of BF compounds in DCM at 3µM concentration.

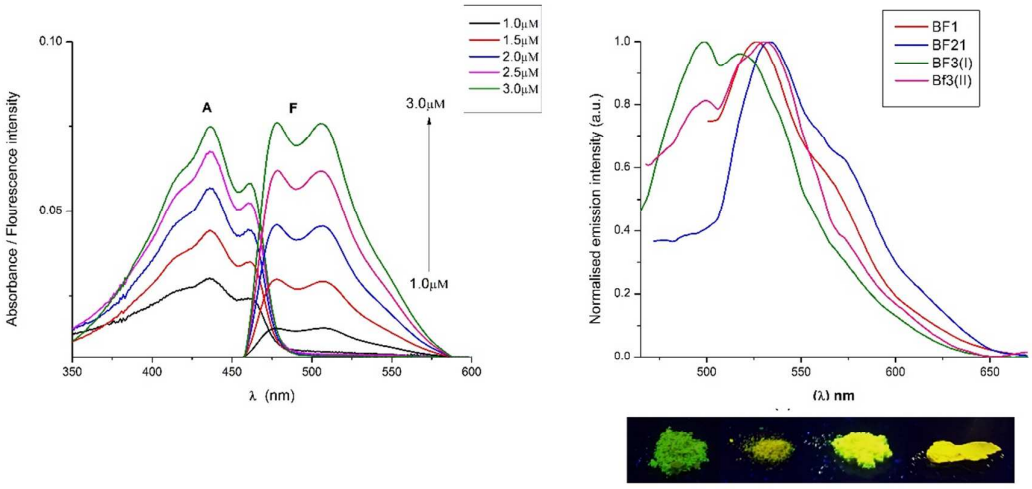

Figure 4: (a) Normalised absorption (A) and fluorescence spectra (F) of compound BF21 in acetone solution at five different concentrations (1) 1 µM (2) 1.5 µM (3) 2.0 µM (4) 2.5 µM (5) 3.0 µM with λ_{Ex} = 434 nm.

(b) Normalised emission spectra of BF Compounds in solid state.

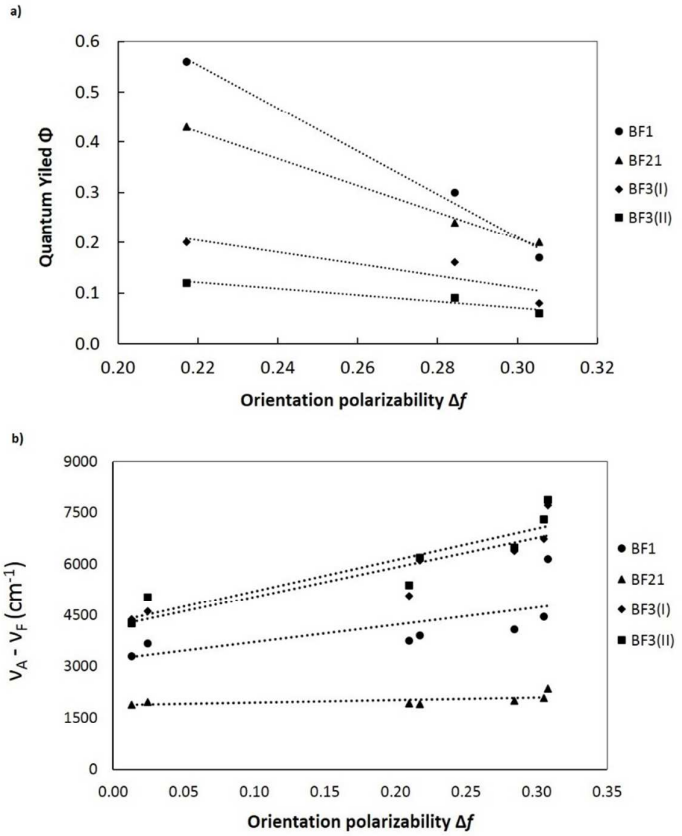

Fig5: (a) Plot of Φ_F v/s (Δf) of BF compounds (DCM, Acetone, Acetonitrile). (b) Plot of Stokes shift ($\nu_A - \nu_F$) v/s solvent polarizability (Δf) of BF compounds in various solvents.

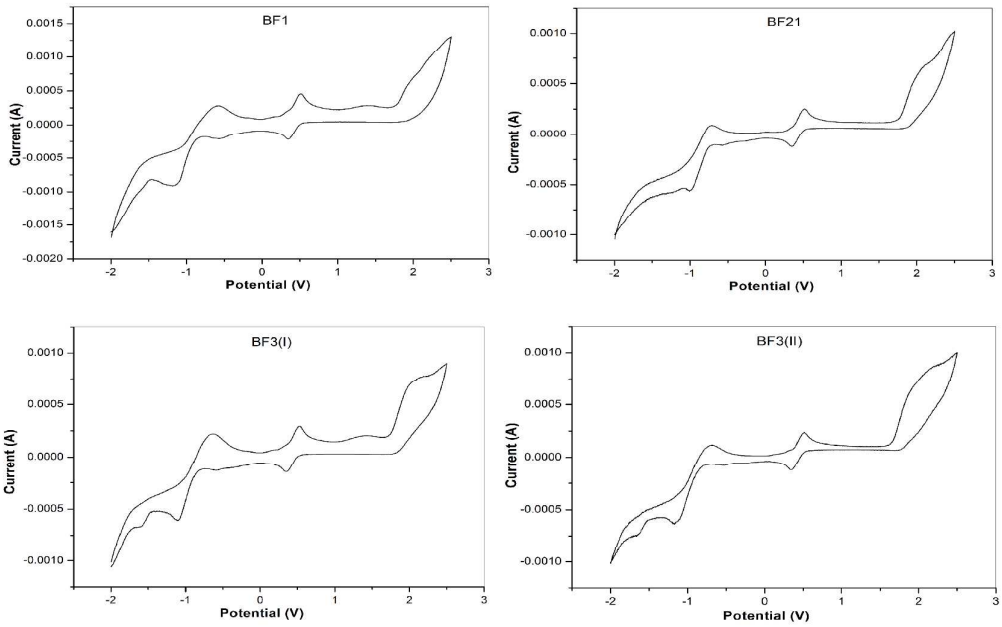

Figure 6: Cyclic voltammograms of BF compounds measured in DCM solution, containing 0.1 M $TBAPF_6$ at 20°C. Ferrocene was used as an internal standard, and potential was calculated relative to the SCE assuming $E_{1/2}$ (Fc/Fc^+) to be +0.43.

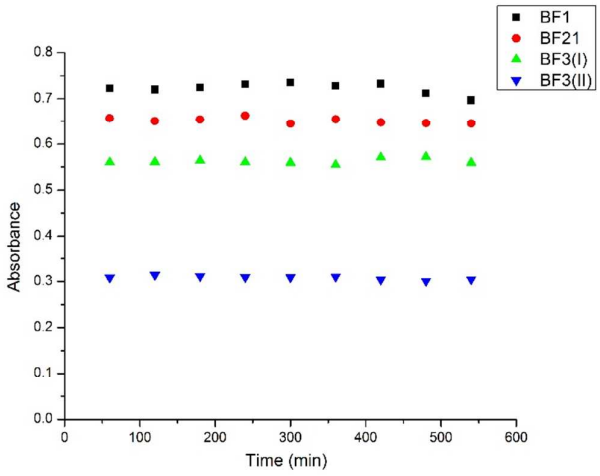

Figure 7: Change in optical density of BF compounds v/s time (min) on irradiation with UV light (0.025W/cm^2).

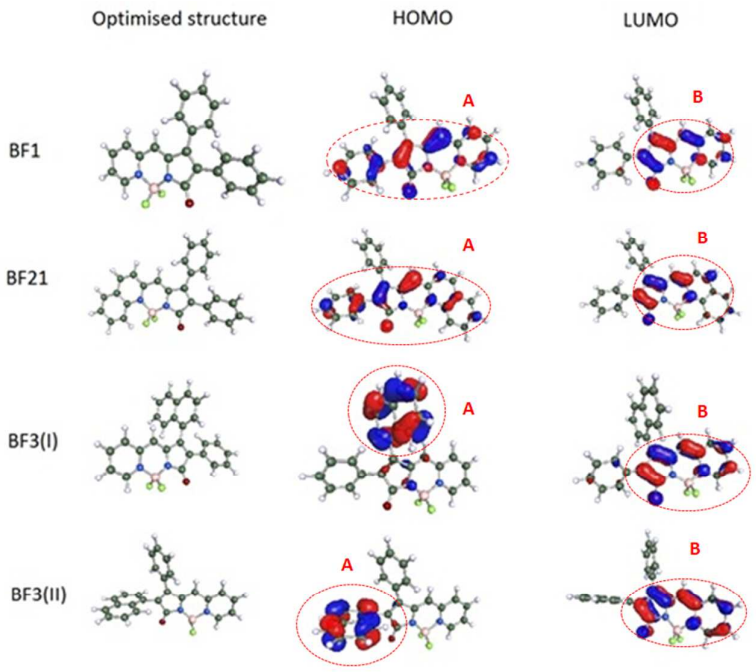

Figure 8: Diagram showing HOMO and LUMO level of BF compounds.

Table 1: Optical properties of BF compounds.

Table 2: Quantum yield (Φ_F), energy yield fluorescence (E_F) of BF compounds in different solvents (DCM, Acetone, Acetonitrile) and fluorescence lifetime (τ) in DCM.

.

Table 3: Ground state and excited state dipole moment difference ($\mu_E - \mu_G$) of BF compounds.

Table 4: Electronic states (HOMO/LUMO levels) values and energy gap (eV).

Table 1: Optical properties of BF compounds.

Compound	Solvent	λ_{ab} (nm)	ε_{max} (M^{-1} cm^{-1})	λ_F (nm)	ν_A - ν_F (cm^{-1})	f
BF1	Toluene	410	23100	474	3293	0.44
	Dioxane	404	37600	474	3655	0.66
	THF	404	30800	476	3744	0.61
	DCM	403	40700	478	3893	0.77
	Acetone	400	36600	478	4079	0.73
	ACN	395	26000	479	4440	0.49
	Methanol	394	84000	520	6150	1.80
BF21	Toluene	445	42100	486	1895	0.66
	Dioxane	442	43700	484	1963	0.38
	THF	441	37700	482	1928	0.65
	DCM	439	33500	479	1902	0.54
	Acetone	436	40300	478	2015	0.69
	ACN	434	30400	477	2077	0.62
	Methanol	432	46100	481	2358	1.08
BF3(I)	Toluene	411	55200	501	4370	1.27
	Dioxane	407	19300	501	4609	0.37
	THF	404	27300	508	5067	0.76
	DCM	402	36900	533	6113	0.73
	Acetone	400	33800	537	6378	0.68
	ACN	401	26800	549	6722	0.52
	Methanol	395	49200	568	7710	1.41
BF3(II)	Toluene	413	21900	501	4252	0.38
	Dioxane	406	38100	510	5022	0.88
	THF	405	31400	518	5386	0.59
	DCM	402	29400	535	6184	0.54
	Acetone	399	24500	538	6475	0.46
	ACN	396	30000	557	7299	0.59
	Methanol	395	16700	573	7864	0.34

Table 2: Quantum yield (Φ_F), energy yield fluorescence (E_F) of BF compounds in different solvents (DCM, Acetone, Acetonitrile) and fluorescence lifetime (τ) in DCM.

Compound	Solvent	Φ_F	E_F	τ(ns)
BF1	DCM	0.56	0.48	1.86
	Acetone	0.30	0.25	
	ACN	0.17	0.14	
BF21	DCM	0.54	0.43	1.23
	Acetone	0.27	0.24	
	ACN	0.45	0.20	
BF3(I)	DCM	0.26	0.20	2.86
	Acetone	0.22	0.16	
	ACN	0.11	0.08	
BF3(II)	DCM	0.16	0.12	1.08
	Acetone	0.12	0.09	
	ACN	0.09	0.06	

Table 3: Ground state and excited state dipole moment difference $(\mu_E - \mu_G)$ of BF compounds.

Compound	Slope	Onsager radius (A°)	$(\mu_E - \mu_G)$ D
BF_1	1779.00	7.05	0.78
BF_2	270.00	7.58	0.34
BF_3(I)	3079.00	7.69	1.18
BF_3(II)	3255.00	7.66	1.20

Table 4: Electronic states (HOMO/LUMO levels) values and energy gap (eV).

Compound	LUMO (eV)		HOMO (eV)		E_g (eV)		
	V_{cv}	V_{ca}	V_{cv}	V_{ca}	V_{cv}	V_{ca}	V_{uv}
BF1	-2.86	-2.84	-6.16	-6.13	3.29	3.29	2.68
BF21	-3.26	-3.04	-6.15	-6.15	2.88	3.11	2.54
BF3(I)	-2.90	-2.95	-6.10	-6.06	3.20	3.11	2.78
BF3(II)	-2.84	-2.81	-6.02	-6.05	3.18	3.24	2.67

V_{cv}: Value from cyclic voltammetry; V_{ca}: Value from MO calculation; V_{uv} = Value obtained from UV-vis absorption edge studies.